Langmuir



Article

# Reversible Gelation of Rod-Like Viruses Grafted with Thermoresponsive Polymers

Zhenkun Zhang, Naveen Krishna, M. Paul Lettinga, Jan Vermant, and Eric Grelet

*Langmuir*, **2009**, 25 (4), 2437-2442• DOI: 10.1021/la8029903 • Publication Date (Web): 23 January 2009



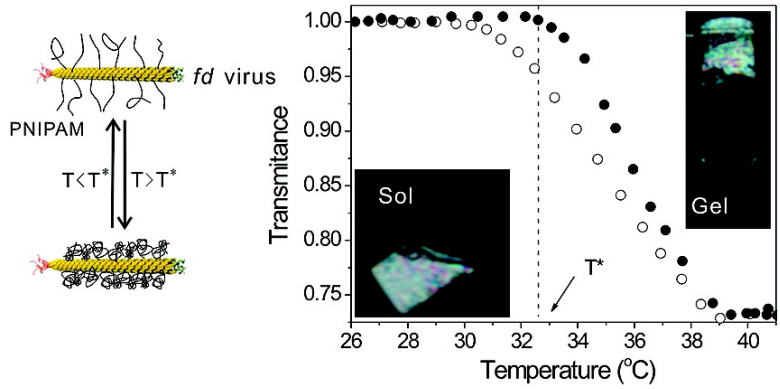


## More About This Article

Additional resources and features associated with this article are available within the HTML version:

- Supporting Information
- Access to high resolution figures
- Links to articles and content related to this article
- Copyright permission to reproduce figures and/or text from this article

View the Full Text HTML

# Reversible Gelation of Rod-Like Viruses Grafted with Thermoresponsive Polymers

Zhenkun Zhang,[†,‡] Naveen Krishna,[§] M. Paul Lettinga,*[,†] Jan Vermant,[§] and Eric Grelet*[,‡]

*IFF, Institut Weiche Materie, Forschungszentrum Jülich, D-52425 Jülich, Germany, Centre de Recherche Paul Pascal, CNRS-Université Bordeaux 1, 115 Avenue Schweitzer, F-33600 Pessac, France, and Department of Chemical Engineering, K.U. Leuven, W. de Croylaan 46, B-3001 Leuven, Belgium*

*Received September 11, 2008. Revised Manuscript Received October 29, 2008*

The synthesis and selected macroscopic properties of a new model system consisting of poly(*N*-isopropylacrylamide) (PNIPAM)-coated rod-like *fd* virus particles are presented. The sticky rod-like colloids can be used to study effect of particle shape on gelation transition, the structure and viscoelasticity of isotropic and nematic gels, and to make both open isotropic as well as ordered nematic particle networks. This model system of rod-like colloids, for which the strength of attraction between the particles is tunable, is obtained by chemically grafting highly monodisperse rod-like *fd* virus particles with thermoresponsive polymers, e.g. PNIPAM. At room temperature, suspensions of the resulting hybrid PNIPAM-*fd* are fluid sols which are in isotropic or liquid crystalline phases, depending on the particle concentration and ionic strength. During heating/cooling, the suspensions change reversibly between sol and gel state near a critical temperature of ∼32 °C, close to the lower critical solution temperature of free PNIPAM. The so-called nematic gel, which exhibits a cholesteric feature, can therefore be easily obtained. The gelation behavior of PNIPAM-*fd* system and the structure of the nematic gel have been characterized by rheology, optical microscopy and small-angle X-ray scattering.

## Introduction

Particle shape has been recognized as an important factor in the understanding and design of colloidal gels and glasses[1,2] that are ubiquitous in industrial applications and biological systems.[3] While the gelation behavior of *spherical* colloids has been intensively investigated,[4] experimental and theoretical studies concerning gelled systems of *anisotropic* particles remain limited[2] mainly because of the lack of suitable model systems. Some rod-like particles or polymers such as boehmite rods,[5] vanadium pentoxide ribbons,[6] worm-like micelles,[7] F-Actin,[8] microtubules,[9] and rigid polypeptide-poly($\gamma$-benzyl-L-glutamate) (PBLG)[10] can gel, but they inherently suffer from polydispersity and irregular or ill defined surface properties. Consequently, the complex interplay between particle shape, interparticle interactions, and gelation behavior is difficult to rationalize. In addition, gelation of these systems occurs in an uncontrollable and often irreversible way because extreme conditions are often required, including high ionic strength,[5] volatile organic solvents,[10] and strong interparticle attractions,[6] which do not allow for a subtle control of the interaction potential and which make systematic investigations difficult to perform. A good model system that is simple and easy to handle and that can gel reversibly under mild conditions is highly relevant.

Besides the intriguing rheological behavior introduced by the anisotropy of the shape, the gelation of anisotropic particles often results in so-called lyotropic nematic gels (LNGs) which combine the spatial particle ordering of the nematic liquid crystals and the elasticity of a physical gel. This kind of gel with nematic ordering has been observed with rod-like (bio)polymers,[11] micelles, and mineral colloids.[5,6] Small organic gelators can also form nematic gels by self-assembly into rod-like microfibrils.[12] Similarly, LNGs are easily formed by intermediate peptide fibrils as observed in the self-assembly of synthetic peptide oligomers, which have been widely explored recently because of their similarity to amyloids characteristic of Alzheimer's and prion diseases.[13] Furthermore, LNGs have other potential applications as scaffolds for nanomaterials, matrices for separation of chiral molecules, and orientational templates for biomolecules used

* Corresponding authors. E-mail: grelet@crpp-bordeaux.cnrs.fr, p.lettinga@fz-juelich.de.

† IFF.

‡ Centre de Recherche Paul Pascal.

§ K.U. Leuven.

(1) (a) Glotzer, S. C.; Solomon, M. J. *Nat. Mater.* **2007**, *6*, 557–562. (b) ten Brinke, A. J. W.; Bailey, L.; Lekkerkerker, H. N. W.; Maitland, G. C. *Soft Matter* **2007**, *3*, 1145–1162. (c) ten Brinke, A. J. W.; Bailey, L.; Lekkerkerker, H. N. W.; Maitland, G. C. *Soft Matter* **2008**, *4*, 337–348.

(2) Philipse, A. P.; Wierenga, A. M. *Langmuir* **1998**, *14*, 49–54.

(3) For recent reviews, see (a) Zaccarelli, E. *J. Phys. Condens. Matter* **2007**, *19*, 323101–323150. (b) Cipelletti, L.; Ramos, L. *J. Phys.- Condens. Matter* **2005**, *17*, R253−R285.

(4) As examples, see (a) Lu, P. J.; Zaccarelli, E.; Ciulla, F.; Schofield, A. B.; Sciortino, F.; Weitz, D. A. *Nature* **2008**, *453*, 499–503. (b) Royall, C. P.; Williams, S. R.; Ohtsuka, T.; Tanaka, H. *Nat. Mater.* **2008**, *7*, 556–561. (c) Campbell, A. I.; Anderson, V. J.; van Duijneveldt, J. S.; Bartlett, P. *Phys. Rev. Lett.* **2005**, *94*, 208301. (d) Pham, K. N.; Puertas, A. M.; Bergenholtz, J.; Egelhaaf, S. U.; Moussaid, A.; Pusey, P. N.; Schofield, A. B.; Cates, M. E.; Fuchs, M.; Poon, W. C. K. *Science* **2002**, *296*, 104–106. (e) Lin, M. Y.; Lindsay, H. M.; Weitz, D. A.; Ball, R. C.; Klein, R.; Meakin, P. *Nature* **1989**, *339*, 360–362.

(5) (a) Mohraz, A.; Solomon, M. J. *J. Colloid Interface Sci.* **2006**, *300*, 155–162. (b) van Bruggen, M. P. B.; Lekkerkerker, H. N. W. *Langmuir* **2002**, *18*, 7141–7145. (c) Wierenga, A.; Philipse, A. P.; Lekkerkerker, H. N. W. *Langmuir* **1998**, *14*, 55–65.

(6) (a) Pelletier, O.; Davidson, P.; Bourgaux, C.; Coulon, C.; Regnault, S.; Livage, J. *Langmuir* **2000**, *16*, 5295–5303. (b) Pelletier, O.; Davidson, P.; Bourgaux, C.; Livage, J. *Europhys. Lett.* **1999**, *48*, 53–59. (c) Pelletier, O.; Bourgaux, C.; Diat, O.; Davidson, P.; Livage, J. *Eur. Phys. J. B* **1999**, *12*, 541–546.

(7) Ryu, J. H.; Lee, M. *J. Am. Chem. Soc.* **2005**, *127*, 14170–14171.

(8) Gardel, M. L.; Shin, J. H.; MacKintosh, F. C.; Mahadevan, L.; Matsudaira, P.; Weitz, D. A. *Science* **2004**, *304*, 1301–1305.

(9) Lin, Y. C.; Koenderink, G. H.; MacKintosh, F. C.; Weitz, D. A. *Macromolecules* **2007**, *40*, 7714–7720.

(10) Uematsu, I.; Uematsu, Y. *Adv. Polym. Sci.* **1984**, *59*, 37–73.

(11) (a) Tadmor, R.; Khalfin, R. L.; Cohen, Y. *Langmuir* **2002**, *18*, 7146–7150. (b) Schmidtke, S.; Russo, P.; Nakamatsu, J.; Buyuktanir, E.; Turfan, B.; Temyanko, E.; Negulescu, L. *Macromolecules* **2000**, *33*, 4427–4432.

(12) Terech, P.; Weiss, R. G. *Chem. Rev.* **1997**, *97*, 3133–3159.

(13) (a) Aggeli, A.; Bell, M.; Boden, N.; Keen, J. N.; Knowles, P. F.; McLeish, T. C. B.; Pitkeathly, M.; Radford, S. E. *Nature* **1997**, *386*, 259–262. (b) Aggeli, A.; Nyrkova, I. A.; Bell, M.; Harding, R.; Carrick, L.; Mcleish, T. C. B.; Semenov, A. N.; Boden, N. *Proc. Natl. Acad. Sci.* **2001**, *98*, 11857–11862.

10.1021/la8029903 CCC: $40.75 
Published on Web 01/23/2009

**Scheme 1. Synthesis of *fd* Viruses Grafted with Poly(*N*-isopropylacrylamide) (1) and the Copolymer of *N*-Isopropylacrylamide and *N-tert*-Butylacrylamide (2)**

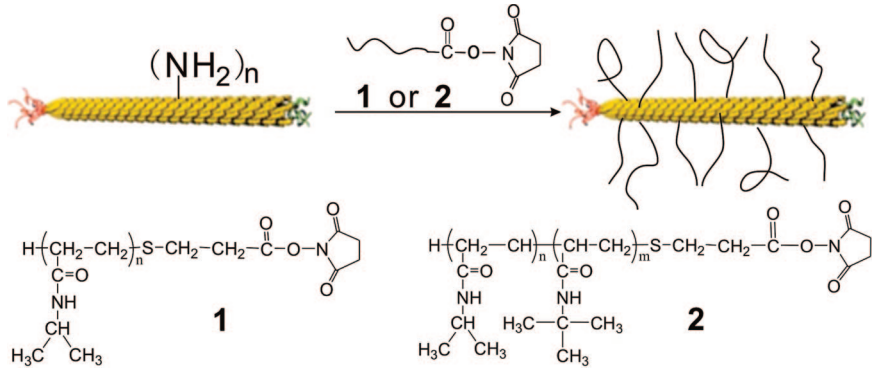


during spectroscopic studies.[14] At the moment, the fundamental questions seem to be how gelation influences the nematic ordering of the component particles and how the nematic ordering affects the viscoelasticity of the subsequent gel. So far, literature focusing on these questions is limited,[6] probably because the formation of the nematic gels, as observed in the aforementioned systems, is usually accompanied by other phenomena such as phase separation,[6] isotropic/nematic transition,[15] and simultaneous self-assembly of the subunits,[13] etc.

In this contribution, a model system of sticky colloidal rods was developed by chemically grafting a thermoresponsive polymer, e.g. poly(*N*-isopropylacrylamide), onto highly monodisperse *fd* virus particles (Scheme 1). The *fd* virus is a rod-like particle with a length of 880 nm, a diameter of 6.6 nm, and a persistence length of 2200 nm. Each virus consists of a capsid of 2700 identical major coat proteins which are arranged helically along the long axis of the virus. This virus has been used both as a model colloidal rod and as a template for nanomaterials, because of its intrinsic monodispersity and well-defined surface properties.[16,17] Chemical modifications such as dye labeling and polymer grafting can be applied to this virus by exploiting its rich surface functional groups.[18] This virus shows robust thermal stability until 90 °C.[19] The thermoresponsive polymer adopted here is the well-documented poly(*N*-isopropylacrylamide) (PNIPAM), a polymer which undergoes a sharp, thermoinduced reversible change from coil to globular conformation at a lower critical solution temperature ($T_{LCST}$, ~32 °C).[20] Here we demonstrate that when PNIPAM is chemically tethered onto the rod-like *fd* virus surface, the resulting hybrid PNIPAM−*fd* exhibits a reversible gelation behavior in aqueous media by simply controlling the temperature. Depending on the ionic strength and particle concentration, both isotropic and nematic gels can be conveniently obtained. Because of the cholesteric nature of the liquid crystalline phase of (PNIPAM)−*fd* suspensions at room temperature,[16] the cholesteric organization is largely preserved in the liquid crystalline gel. This offers an easy way to monitor the evolution of the gel phase and to probe the properties of the (chiral) nematic gel by polarized optical microscopy (POM) and small-angle X-ray scattering (SAXS). Measurements of the linear viscoelastic properties as a function of temperature and frequency have been used to obtain an accurate determination of the gel point.

## Results and Discussion

**Grafting *fd* Virus with Thermoresponsive Polymer.** *fd* virus can be grown and collected in hundreds of milligrams following standard biochemical protocols using the XL-1 blue strain of *E. coli* as the host bacteria.[21] Poly(*N*-isopropylacrylamide) (PNIPAM) oligomer and the copolymer of *N*-isopropylacrylamide (NIPAM) and *N-tert*-butylacrylamide (NBA) (polymer **1** and **2** in Scheme 1), both of which contain a carboxyl group at one end, were synthesized by radical polymerization with AIBN as the initiator and 3-mercaptopropionic acid (MPA) as the chain transfer agent.[22] The carboxyl end groups are introduced by MPA and converted into the succinimidyl ester by esterification with *N*-hydroxysuccunimide after activation with *N,N*-dicyclohexylcarbodiimide. The activated polymer was then grafted to the surface of *fd* virus through the reaction of the end succinimidyl group of the polymers with the amino groups on the protein surface of the viruses. About 300 polymer chains with a number average molecular weight ($M_n$) of 7k were grafted onto each rod, corresponding to a grafting density of 0.1 PNIPAM/nm$^2$. This amount of PNPAM is sufficient to completely cover the virus surface.[23] An extensive purification procedure was applied to remove any free polymer.[24] PNIPAM−*fd* was subjected to different experiments, while only gel point determination was performed on *fd* grafted with the copolymer **2**.[24]

**Phase Behavior of PNIPAM−*fd* at Room Temperature.** Rod-like particles like *fd* viruses are well-known to form concentration-dependent liquid crystalline phases (LC).[16,25] The isotropic/nematic (I/N) phase transition of *fd* virus follows Onsager's theory and the concentration, $C_{I-N}$, at which an I/N transition occurs, increases as a function of the ionic strength ($I$) as $1/D_{eff}^{electrostatic}$, where $D_{eff}^{electrostatic}$ is an effective diameter defined

(14) (a) Clore, G. M.; Starich, M. R.; Gronenborn, A. M. *J. Am. Chem. Soc.* **1998**, *120*, 10571–10572. (b) Sass, H. J.; Musco, G.; Stahl, S. J.; Wingfield, P. T.; Grzesiek, S. *J. Biomol. NMR* **2000**, *18*, 303–309.

(15) Michot, L. J.; Bihannic, I.; Maddi, S.; Funari, S. S.; Baravian, C.; Levitz, P.; Davidson, P. *Proc. Natl. Acad. Sci. U.S.A.* **2006**, *103*, 16101–16104.

(16) Dogic, Z.; Fraden, S. In *Soft Matter-Complex Colloidal Suspensions*; Gompper, G., Schick, M., Eds.; Wiley-VCH: Weinheim, Germany, 2006; Vol. *2*, pp 1−86, and references therein.

(17) (a) Nam, K. T.; Kim, D. W.; Yoo, P. J.; Chiang, C. Y.; Meethong, N.; Hammond, P. T.; Chiang, Y. M.; Belcher, A. M. *Science* **2006**, *312*, 885–888. (b) Lee, S. W.; Lee, S. K.; Belcher, A. M. *Adv. Mater.* **2003**, *15*, 689–692. (c) Zhang, Z. K.; Buitenhuis, J. *Small* **2007**, *3*, 424–428.

(18) (a) Dogic, Z.; Fraden, S. *Philos. Trans. R. Soc. Lond., Ser. A* **2001**, *359*, 997–1014. (b) Lettinga, M. P.; Barry, E.; Dogic, Z. *Europhys. Lett.* **2005**, *71*, 692–698. (c) Lettinga, M. P.; Grelet, E. *Phys. Rev. Lett.* **2007**, *99*, 197802.

(19) Wen, Q.; Tang, J. X. *Phys. Rev. Lett.* **2006**, *97*, 048101.

(20) Schild, H. G. *Prog. Polym. Sci.* **1992**, *17*, 163–249.

(21) Sambrook, J.; Russell, D. W. *Molecular Cloning: A Laboratory Manual*; 3rd ed.; Cold Spring Harbor Laboratory Press: New York, 2001.

(22) (a) Chen, G.; Hoffamn, A. S. *J. Biomater. Sci. Polym. Ed.* **1994**, *5*, 371–382. (b) Takei, Y. G.; Aoki, T.; Sanui, K.; Ogata, N.; Okano, T.; Sakurai, Y. *Bioconjugate Chem.* **1993**, *4*, 42–46.

(23) Grelet, E.; Fraden, S. *Phys. Rev. Lett.* **2003**, *90*, 198302.

(24) See Supporting Information.

(25) Grelet, E. *Phys. Rev. Lett.* **2008**, *100*, 168301.

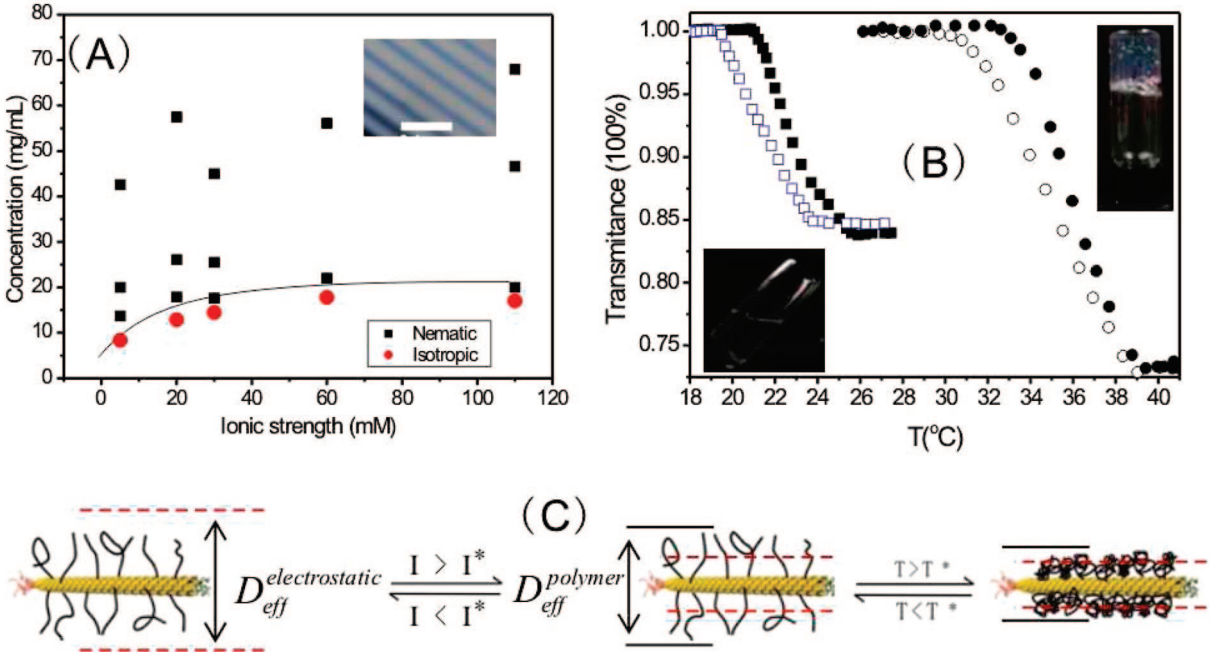


**Figure 1.** (A) Phase diagram of PNIPAM−*fd* system at room temperature (in the sol state). The line is only to guide the eye. Full circles refer to the highest measured concentrations where the isotropic liquid phase is still observed. Solid squares represent concentrations where the (chiral) nematic phase is observed. Inset: Typical fingerprint texture of the cholesteric phase observed by optical microscopy between crossed polarizers in a suspension of $I = 5$ mM, $C = 20$ mg mL$^{-1}$ (the scale bar indicates 100 $\mu$m). (B) Transmittance versus temperature during reversible gelation of the suspensions of *fd* virus grafted with the thermoresponsive polymer **1** (circles) or **2** (squares). Full symbols: heating; open symbols: cooling. The virus concentration is 3.5 mg mL$^{-1}$ (in isotropic liquid phase at room temperature, $I = 110$ mM); the heating/cooling speed is 1 °C per 30 min. Inset: sol and gel of *fd* viruses grafted with polymer **1**. (C) Schematic representation of the different effective diameters and their variation upon changing experimental conditions. Black line: $D_{eff}^{polymer}$; red dash line: $D_{eff}^{electrostatic}$; *I*: ionic strength with $I^* \sim 20$ mM; *T*: temperature with $T^* \sim 32$ °C.

by the surrounding electrical double layer (Figure 1C).[23] At physiological pH, *fd* virus bears a high negative surface charge density (∼10 e/nm),[26] resulting in strong electrostatic repulsions which lead to the colloidal stability of the virus suspensions. For polymer−*fd* systems, an additional soft-repulsion is introduced by the grafted polymer layer in good solvents. Above a given ionic strength *I*, the electrical double layer is confined underneath the polymer layer and the effective diameter of the hybrid rods is defined solely by the thickness of the grafted polymer ($D_{eff}^{polymer}$, Figure 1C). $C_{I-N}$ becomes then independent of *I*, as revealed by the phase behavior of *fd* grafted with poly(ethylene glycol) (PEG) of molecular weight 5k (PEG5k−*fd*).[23] Determination of the I/N transition for the current PNIPAM−*fd* suspensions at room temperature evidence that $C_{I-N}$ varies for $I < 20$ mM while it is essentially independent of *I* for $I > 20$ mM (Figure 1A), which is very similar to PEG5k−*fd*. $C_{I-N} \sim 17$ mg mL$^{-1}$ is found for $I = 110$ mM and this is much lower than bare *fd* (∼24−25 mg mL$^{-1}$) and close to PEG5k−*fd* (∼15 mg mL$^{-1}$) at the same ionic strength.[23]

Similar to PEG5k−*fd* and bare *fd*, the mesophase observed for the current system is a cholesteric phase in which the director (average rod orientation) follows a helical path in space, resulting in a characteristic stripe-like "fingerprint" texture (inset of Figure 1A). We also noted that pure nematic phases are observed in some samples especially at high rod concentrations and ionic strengths, in contrast with PEG5k−*fd* and bare *fd* for which only the cholesteric phase is observed. The origin of this pure nematic phase might be related to slow particle reordering in the liquid crystalline phase or interactions between the grafted PNIPAM layers. A systematic investigation of these phenomena is being carried out since this might shed some light about the origin of the supramolecular helical organization of *fd* virus[23,27] and many other rigid macromolecules such as DNA,[28] rod-like polypeptides,[10] and celluloses.[29]

**Reversible Gelation of *fd* Grafted with Thermoresponsive Polymers.** Upon heating above a critical temperature, *T**, the PNIPAM−*fd* suspension undergoes a sharp transition from a sol to a gel as inferred from the light transmittance and the mechanical properties of the system (Figure 1B). The gelation is *reversible*, and the gel turns back to a fluid state by decreasing the temperature. From the test tube inversion method and the measurement of the transmittance, *T** is estimated to be in the temperature range of 32−35 °C, close to $T_{LCST}$ for the free PNIPAM (Figure 1B).[7]

For $T > T^*$, the role of the grafted PNIPAM on *fd* surface changes as PNIPAM chains shrink into globular conformation and their hydrophobic nature dominates interparticle interactions (Figure 1C). The strong hydrophobic attraction between the collapsed PNIPAM layers drives the system into the gel state, even in salt free suspensions above a concentration of 2 mg mL$^{-1}$. This indicates a strong interparticle attraction when $T > T^*$. The critical concentration, *C**, above which space-filling gel forms, weakly decreases with increasing ionic strength, as for instance when $I = 110$ mM, *C** is found to be 1 mg mL$^{-1}$.[24] The corresponding minimum effective volume fraction for gelation, $\phi^*$, is estimated to be 0.002 by assuming the effective diameter

(26) Zimmermann, K.; Hagedorn, H.; Heuck, C. C.; Hinrichsen, M.; Ludwig, H. *J. Biol. Chem.* **1986**, *261*, 1653–1655.

(27) (a) Tombolato, F.; Ferrarini, A.; Grelet, E. *Phys. Rev. Lett.* **2006**, *96*, 258302. (b) Tomar, S.; Green, M. M.; Day, L. A. *J. Am. Chem. Soc.* **2007**, *129*, 3367–3375. (c) Kohlstedt, K. L.; Solis, F. J.; Vernizzi, G.; de la Cruz, M. O. *Phys. Rev. Lett.* **2007**, *99*, 030602.

(28) Stanley, C. B.; Hong, H.; Strey, H. H. *Biophys. J.* **2005**, *89*, 2552–2557.

(29) Revol, J.-F.; Godbout, L.; Dong, X.-M.; Gray, D. G. *Liq. Cryst.* **1994**, *16*, 127–134.

($D_{eff}$) of the PNIPAM−*fd* in gel phase (Figure 1C), $D_{eff} = D_{bare} + 4R_g$, in which $D_{bare}$ is the diameter of bare *fd* (6.6 nm) and $R_g$ is the radius of gyration of the collapsed PNIPAM (with $R_g$ estimated to be 1 nm for collapsed PNIPAM of $M_n$ 7k[30]). For other rod systems, $\phi^* > 0.003$ has been reported.[5,6] The somewhat lower $\phi^*$ of PNIPAM−*fd* benefits from its much longer contour length.

The gelation temperature can be tuned by grafting a copolymer of NIPAM with other hydrophobic or hydrophilic monomers. For example, the copolymer of NIPAM and *N-tert*-butylacrylamide (polymer **2** in Scheme 1) has $T_{LCST}$ ~22 °C and the $T^*$ of *fd* grafted with polymer **2** is observed to be about ~21 °C (Figure 1B).[24] Note that some hysteresis in the heating/cooling cycle is observed for both systems (Figure 1B), which is attributable to the hysteresis inherent in the thermoreversible behavior of polymer **1** or **2**.[31] The appearance of the gel varies from translucent to turbid with increasing concentration. The gel formed at particle concentrations below 30 mg mL$^{-1}$ remains sufficiently transparent to visible light to allow for the investigation of the gelation with polarized optical microscopy (POM).

**Rheological Characterization of Gelation Behavior of PNIPAM−*fd* Suspensions.** Dynamic oscillatory experiments were performed on PNIPAM−*fd* suspensions at different temperatures in the linear viscoelastic region. Concerning the definition of a gel, the Winter and Chambon method was adopted (see Supporting Information for a brief description of this method and terminology).[32] Thermally induced gelation is compared for two samples with the same virus concentration, 8.5 mg mL$^{-1}$, but at two different ionic strengths $I = 5$ mM and 110 mM.

At $I = 5$ mM, the suspension is in the cholesteric liquid crystalline phase and birefringence is observed between crossed polarizers when $T < T^*$ (inset in Figure 3A), whereas at $I = 110$ mM the system is in the isotropic liquid phase. In this way, two systems with the same particle number density but with a different microstructure are realized by simply varying the ionic strength. This structure difference is clearly responsible for the different rheological behavior of the two suspensions ($T < T^*$), as summarized in Figure 2. Before gelation, the storage modulus $G'$ and loss modulus $G''$ of the suspension at $I = 110$ mM is dependent on the frequency ($\omega$) as $G'(G'') \sim \omega^n$ with $n \sim 0.5$, which is in a good agreement with theory.[32] In contrast, a less regular tendency is observed for $I = 5$ mM, probably because of the existence of polydomains in the liquid crystalline phase. Above a critical temperature, $G'$ and $G''$ of both systems become independent of frequency, with $G'$ higher than $G''$, which is a typical feature of gels.[32] The critical temperature at which gelation occurs, $T^*$, can be deduced following Winter and Chambon method.[24,32] $T^* = 35.2$ and 33.2 °C are obtained for the suspension at $I = 5$ and 110 mM, respectively, which provide a more accurate measure compared to the value obtained by the test tube inversion method.

Further investigation reveals that at the same frequency, the storage modulus $G'$ of the suspension at $I = 5$ mM (in nematic phase) is higher than at $I = 110$ mM (in isotropic liquid phase) before gelation while opposite trend is observed after gelation (Figure 2C). The weaker screening of the electrostatic interactions of rods at $I = 5$ mM leads to a larger effective diameter and hence a higher effective particle volume fraction than at $I = 110$ mM (Figure 1C). This results in a higher modulus of the suspension at $I = 5$ mM in the sol state. As detailed in the following section, the gel at $I = 5$ mM is indeed a nematic gel with an oriented network which may yield to applied stress more easily than the random entangled network at $I = 110$ mM.

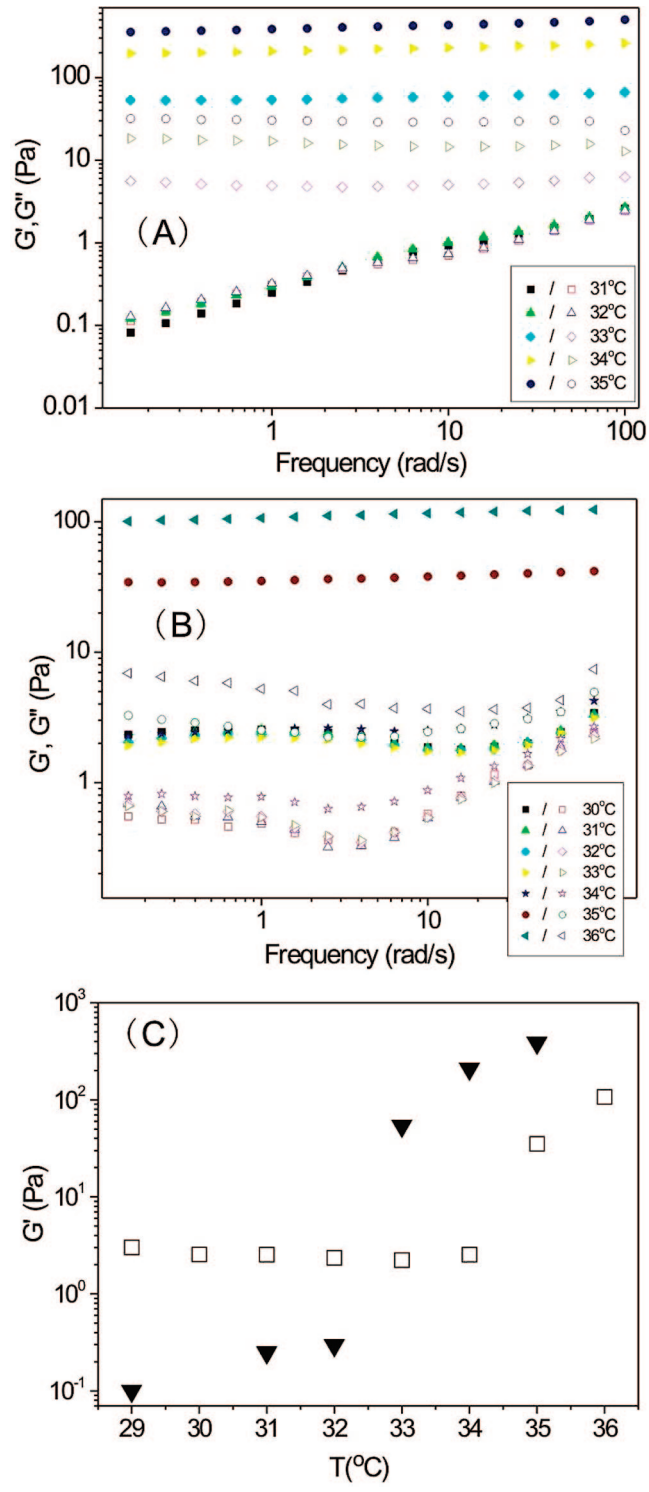


**Figure 2.** Dynamic frequency sweep experiments at different temperatures of two PNIPAM−*fd* suspensions at the same virus concentration, $C = 8.5$ mg mL$^{-1}$, but at different ionic strengths of $I = 110$ mM and at $I = 5$ mM. They are in the isotropic liquid and nematic phases, respectively. (A) $I = 110$ mM and at a strain of 2.5%, (B) $I = 5$ mM and at a strain of 0.8%. Full symbols: storage modulus $G'$; open symbols: loss modulus $G''$. (C) Storage modulus ($G'$) as a function of temperature, recorded at a frequency of 1 rad s$^{-1}$. Full triangles: sample at $I = 110$ mM; open squares: sample at $I = 5$ mM.

(30) Wu, C.; Wang, X. H. *Phys. Rev. Lett.* **1998**, *80*, 4092.
(31) (a) Cheng, H.; Shen, L.; Wu, C. *Macromolecules* **2006**, *39*, 2325–2329. (b) Zhu, P. W.; Napper, D. H. *J. Colloid Interface Sci.* **1996**, *177*, 343–352.
(32) Chambon, C.; Petrovic, Z. S.; MacKnight, W. J.; Winter, H. H. *Macromolecules* **1986**, *19*, 2146–2149.

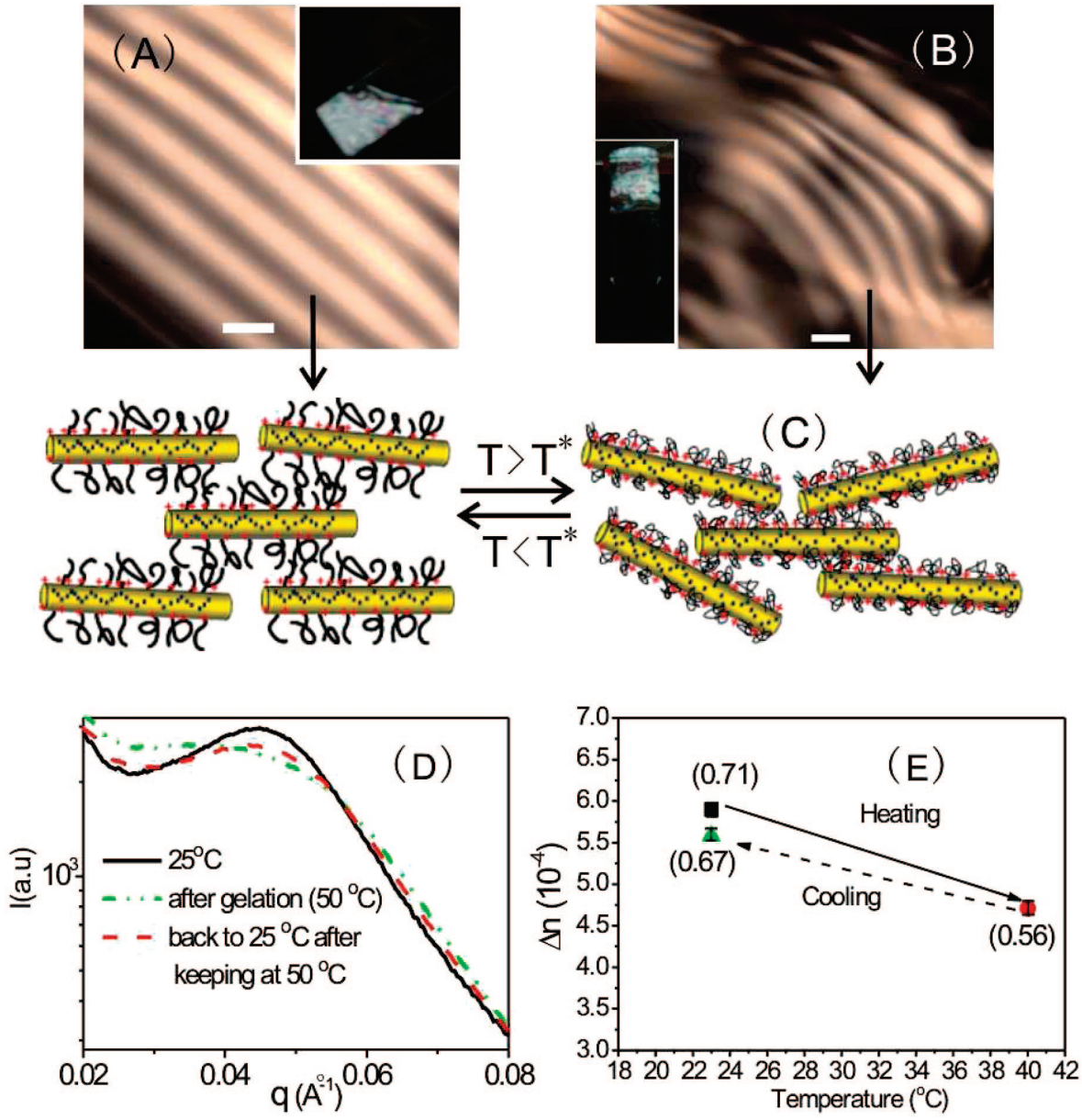


**Figure 3.** (A and B): Fingerprint texture characteristic of the cholesteric phase observed by polarizing microscopy before and after gelation. Dark lines correspond to regions where the rods are perpendicular to the plane of the figure and bright lines correspond to regions where rods are in the plane of figure. The cholesteric pitch corresponds to two bright and two dark lines. The scale bar indicates 100 $\mu$m. Sample: $I = 5$ mM, $C = 13.6$ mg mL$^{-1}$. Inset: Observation of the sol and gel between crossed polarizers. (C) Schematic representation of the rod orientation in the sol and gel states. (D) Intensity versus scattering vector **q** from SAXS experiments at different temperatures. Sample: $I = 110$ mM and $C = 68$ mg mL$^{-1}$. (E) Birefringence $\Delta n$ at different temperatures. Sample: $I = 60$ mM and $C = 22$ mg mL$^{-1}$. The sample was aligned by a magnetic field before heating. Square: $\Delta n$ at room temperature (23 °C) before heating; circle: $\Delta n$ at 40 °C; triangle: $\Delta n$ after cooling back to 23 °C. The values in the parenthesis are the corresponding orientational order parameter $S$.

The above discussions do not take into account the effect of the ionic strength on the $T_{LCST}$ of the free PNIPAM.[33] However, in the range of monovalent salt concentration ($I < 110$ mM) used in this work, any shift in $T_{LCST}$ can be neglected.[33]

**Thermoreversible Liquid Crystalline (LC) Gel of Intriguing Microstructure.** The gel at $I = 5$ mM shows birefringence under cross polarizers (inset of Figure 3B), indicating that a thermoreversible LC gel forms. Thus, the particle ordering in the LC phase at room temperature is maintained during gelation. In addition, if the sol is in the cholesteric phase, the fingerprint texture can still be observed in the gel (Figure 3A,B), within which the helical arrangement of the rods is largely kept. However, investigation of the heating process with POM reveals that the pitch in the gel becomes inhomogeneous (Figure 3B). After cooling back to room temperature, a homogeneous pitch recovers slowly on a time scale of several hours. The inhomogeneous pitch in the gel indicates reordering of the rods and heterogenizing of the inter-rod distance in the nematic gel, although an averaged orientation still exists (Figure 3C). This can also be evidenced with small-angle X-ray scattering (SAXS) measurements (Figure 3D), where the characteristic peak of the nematic phase (structure factor) of anisotropic colloids at room temperature flattens out into a broad peak after gelation. Yet the peak recovers upon cooling.

In a magnetic field, *fd* virus in suspensions can be aligned parallel to the field because of its diamagnetic anisotropy, which

(33) (a) Zhang, Y. J.; Furyk, S.; Bergbreiter, D. E.; Cremer, P. S. *J. Am. Chem. Soc.* **2005**, *127*, 14505–14510. (b) Freitag, R.; Garret-Flaudy, F. *Langmuir* **2002**, *18*, 3434–3440.

offers an easy way to tune the ordering of the particles.[34] By combining this magnetic alignment effect with gelation, one can control the particle ordering in the gel. For this, a suspension of PNIPAM−*fd* was first aligned in a magnetic field of 7 T, resulting in a *monodomain* of pure nematic phase in which all of the rods point to an average direction. The well-oriented sample was removed from the magnetic field and then subjected to the thermal process. Quick heating was adopted, aiming to freeze the monodomain of pure nematic phase and to get LC gels with relatively homogeneous structure. During gelation, the birefringence $\Delta n$ was measured using a Berek compensator (Figure 3E).[24] The orientational order parameter $S$ quantifying the degree of alignment ($-1/2 < S < 1$), is related to $\Delta n$ by $\Delta n/C = S\Delta n_{sat}/C_0$, where $\Delta n_{sat}/C_0$ and $C$ are specific birefringence of perfectly aligned particles and concentration respectively. By assuming that $\Delta n_{sat}/C_0$ of PNIPAM−*fd* is similar to bare *fd* suspensions for which $3.8 \times 10^{-5}$ mL mg$^{-1}$ is reported,[35] the orientational order parameter $S$ can be estimated and the result is included in Figure 3E. Upon heating, $S$ decreases from 0.71 to 0.56, indicating that the alignment in the gel sate decreases but is still maintained to a significant degree. After cooling to room temperature, $S$ increases back to 0.67.

## Summary and Conclusions

End-functionalized thermoresponsive polymers such as poly(*N*-isopropylacrylamide) (PNIPAM) have been synthesized and grafted to rod-like colloidal virus particles. The resulting system combines the thermoresponsiveness of PNIPAM and the perfect monodispersity and rod-like shape of the *fd* virus. This system exhibits reversible gelation behavior upon changing the temperature. The gelation temperature can be tuned by grafting polymers with different lower critical solution temperatures. Isotropic and (chiral) nematic gels are easily obtained by varying the ionic strength or the particle concentration. If the rod-like particles in the suspension are first aligned by magnetic field and then subjected to heating, macroscopically oriented gels can be obtained. Combination of ionic strength, particle concentration, polymer structure, temperature, and magnetic field represents a powerful way to tune the gelation behavior and the resulting properties of the current system. Moreover, because of the monodispersity of the particles, theoretical models can be applied to understand the phase and rheological behaviors.

**Acknowledgment.** This work was supported by the European network of excellence-SoftComp. The EU is also acknowledged for funding through Nanodirect FP7-NMP-2007-SMALL-1, project 213948. We also thank Sabine Willbold for performing NMR measurement and Johan Buitenhuis for useful discussion. Jan K. Dhont is acknowledged for stimulating discussions and for his reading of the manuscript.

**Supporting Information Available:** Synthesis of polymer **1** and **2**, grafting of *fd* viruses with these polymers, test tube inversion, optical microscopy, rheological, and SAXS experiments. This material is available free of charge via the Internet at http://pubs.acs.org.

LA8029903

(34) Torbet, J.; Maret, G. *Biopolymers* **1981**, *20*, 2657–2669.
(35) Purdy, K. R.; Dogic, Z.; Fraden, S.; Ruhm, A.; Lurio, L.; Mochrie, S. G. J. *Phys. Rev. E* **2003**, *67*, 031708.

# Supporting Information

## Reversible Gelation of Rod-like Viruses Grafted with Thermoresponsive Polymers

Zhenkun Zhang,[†, ‡] Naveen Krishna,[§] M. Paul Lettinga,[*,†] Jan Vermant,[§] and Eric Grelet [*,‡]

*IFF, Institut Weiche Materie, Forschungszentrum Jülich, D-52425 Jülich, Germany, Centre de Recherche Paul Pascal, CNRS-Université Bordeaux 1, 115 Avenue Schweitzer, F-33600 Pessac, France, and Department of Chemical Engineering, K.U. Leuven, W. de Croylaan 46, B-3001 Leuven, Belgium*

E-mail: grelet@crpp-bordeaux.cnrs.fr, p.lettinga@fz-juelich.de

### 1. Materials and instrumental

1.1 Materials

All chemicals were obtained from Sigma-Aldrich except otherwise noted. *N*-isopropylacrylamide (NIPAM) was recrystallized from hexane three times; *N-tert*-butylacrylamide (NBA) was recrystallized from 1:1 benzene/acetone three times; 2,2'-Azoisobutyronitrile (AIBN) was recrystallized from ethanol twice. 3-Mercaptopropionic acid (MPA), *N*-hydroxysuccunimide (NHS), *N*,*N*-dicyclohexylcarbodiimide (DCC), *tert*-butylalcohol, anhydrous diethyl ether, methylene chloride were used as received. Other solvents and agents are in the highest purity available commercially and water from a Milli Q system (>18.2 mΩ, Millipore) was used. The buffer mentioned in the text is Tris-HCl buffer (20 mM Tris, pH 8.2), the ionic strength (I) of which was adjusted by adding varying amount of NaCl.

1.2 Instrumental

$^1$H spectra were recorded from $CDCl_3$ solutions on Varian Inova 400 spectrometer. UV spectra were recorded using a Varian Cary 50BIO spectrophotometer. For other instruments, see the respective section.

† IFF, Institut Weiche Materie, Forschungszentrum Jülich.
‡ Centre de Recherche Paul Pascal, CNRS-Université Bordeaux 1.
§ Department of Chemical Engineering, K.U. Leuven.

## 2. Synthesis

2.1 Synthesis of end-functionalized polymers

Following the method of Hoffman and Takei,[1] poly(*N*-isopropylacrylamide) oligomer and copolymer of NIPAM and NBA, both of which contain a carboxyl group at one end, were synthesized by radical polymerization with AIBN as the initiator and MPA as the chain transfer agent. The carboxyl end groups are introduced by MPA and converted into succinimidyl ester by esterification with NHS after activation with DCC.

*Carboxyl group terminated poly(N-isopropylacrylamide)*(*PNIPAM,* polymer **1** in the main text) Based on the recipe in ref. 1a, the molar ratio, [NIPAM]:[MPA]:[AIBN] = 100:2:0.25 was used, targeting a molecular weight of ca. 7k. An Erlenmeyer flask was charged with 50 mL *tert*-butylalcohol, to which 11.30 g NIPAM was added. To the resulted solution were added 173 μL MPA and 41 mg AIBN. After AIBN was dissolved, the clear solution was transferred into a Schlenk flask and degassed by freeze-thaw cycles under vacuum for at least three times. The polymerization was carried out at 60$^{o}$C for 6 hrs. After that, the reaction mixture was concentrated by a rotary evaporator and the concentrate was poured into anhydrous diethyl ether. The precipitate was collected by centrifuge at low speed and dried in vacuum. The product was further purified by dissolving in THF and precipitating in diethyl ether for three times followed by a final drying step. A whitish gel-like product was obtained with a yield of 65%, taking into account the lost during purification. The NMR spectrum of the polymer in $CDCl_3$ is consistent with the literature[2].

*Carboxyl group terminated poly(N-isopropylacrylamide-co-N-tert-butylacrylamide)*(*PNIBA,* polymer **2** in the main text) The molar ratio of the monomers, [NIPAM]:[NBA], is 4:1 and the [Monomer]:[MPA]:[AIBN] is 100:2:0.25, targeting also a molecular weight of ca. 7k. A similar procedure as described above was used. Briefly, to 100 mL *tert*-butylalcohol were added 15.60 g NIPAM, 4.40 g NBA, 346 μL MPA and 82 mg AIBN. The resulted solution was degassed for at least three times. The polymerization was carried out at 60$^{o}$C for 6 hrs. The product was purified and collected by dissolving in THF and precipitating in diethyl ether. The dried product is a white loosen chunk. A yield of 52% was estimated. The final oligomer contains ca. 30% NBA, as estimated from $^{1}$H NMR integrals of diagnostic peaks ($(CH_3)_3C$- at 1.31 ppm for NBA and $(CH_3)_2CH$- at 1.12 ppm for NIPAM).

*Activation of the carboxyl terminated polymer with N-hydroxysuccunimide* The above carboxyl terminated polymers (4g) were dissolved in anhydrous methylene chloride (40 mL). The solution was cooled in ice-$H_2O$ bath. NHS (0.23 g, 2 mmol) was added to the cooled solution. After NHS dissolved, 0.412 g (2 mmol) DCC was added. The final solution was slowly warmed to room temperature and kept stirring for 4 hrs. The solid (insoluble dicyclohexylurea) was removed by filtering. The clear filtrate (~ 40 mL) was poured into 200 mL anhydrous diethyl ether. The precipitate was collected by centrifugation and dried under vacuum. White solids were obtained. The presence of NHS ester was confirmed via UV absorption ($\lambda_{max}$ = 259 nm in a 0.1 N $NH_4$·OH solution).[3]

2.2 Grafting *fd* virus with end-functionalized polymers

*Preparation of fd virus* *fd* virus was grown and purified following standard biochemical protocols using the XL-1 blue strain of *E. coli* as the host bacteria.[4] The yield is ca. 15 mg of *fd* per liter of infected bacteria dispersion, and the virus was typically grown in 6 L batches. The virus particles were purified by repeated centrifugation (108,800 *g* for 5 hrs) and finally redispersed in a 10 mM $NaHCO_3$ buffer with 15% (v/v) ethanol and kept refrigerated at +5 $^oC$ to prevent bacteria propagation. Virus suspension was further centrifuged at 5180 *g* for half an hour to remove any potential bacteria right before using. The concentration of the virus suspension was determined photometrically with the extinction coefficient of 3.84 $mg^{-1}$ $cm^2$ at 269 nm[5]. The absorption ratio at 269 nm and 244 nm ($A_{269}/A_{244}$) was used to assess the purity of *fd*. A ratio of 1.41 indicates a rate of impurity less than 1%.[5]

*Grafting fd virus with polymers* Mass ratio of *fd* to the polymer was kept at 1:10 for the maximum grafting density. Due to the slow dissolution of PNIPAM or the copolymer and the vulnerability of NHS ester to hydrolysis, the following protocol was deployed. *Fd* virus was dispersed in phosphate buffer (110 mM, pH = 8.2) to form suspensions of 2 mg $mL^{-1}$. The suspension (10 mL) was cooled in an ice-water bath and then was added to 200 mg activated polymer. The reaction container was kept in the ice-water bath until most of the polymer was dissolved. Finally, the mixture was kept at room temperature overnight.

Careful purification procedure was performed to remove any free polymers. After the above grafting reaction, the mixture was subjected to several rounds of centrifugation/redispersing in the

targeting buffer at 10°C (centrifugation: 108,800 *g* for at least 8 hrs). At each round, the supernatant was collected to monitor the transmittance versus temperature with the homemade scanning Michelson differential interferometer setup in order to detect any residual free polymer (see next section). It was found that no change of the transmittance with temperature can be detected after the fourth round of centrifugation. To be sure, five rounds of centrifugation/redispersing were usually carried out. After this procedure, the suspension was further dialyzed with a cellulose membrane tubling of MWCO 30k (Spectra). Hereafter we refer to *fd* grafted with PNIPAM as PNIPAM-*fd*. PNIPAM-*fd* was subjected to different experiments while only gel point determination was performed on *fd* grafted with PNIBA (PNIBA-*fd*).

## 3. Characterization

3.1 Characterization of the end-functionalized polymers

*Molecular weight* The number average molecular weight ($M_n$) of the carboxyl terminated PNIPAM was estimated by end functional group titration. For this, the carboxyl terminated polymer (0.25 g) was dissolved in water overnight and cooled at 10°C. The solution was titrated with 0.1 *N* NaOH to obtain the molar amount of the carboxyl groups. Then $M_n$ was calculated by assuming that each polymer contains one carboxyl group.[1] $M_n$ ~ 6865 g/mol was obtained. No attempt was preformed to determine the molecular weight distribution of the polymer, which is expected to be moderately narrow since chain transfer polymerization was used.[1]

*Determination of the lower critical solution temperature ($T_{LCST}$) of the carboxyl-terminated polymers* The evolution of the transmittance with temperature of the polymer solutions was monitored on a homemade scanning Michelson differential interferometer with a laser source of 633 nm and a programmable temperature control unit with an accuracy of ±0.01 °C.[6] The carboxyl-terminated polymers were dissolved in water at T = 10°C overnight, resulting in clear solution of 0.06% (m/v). The temperature was increased/decreased by steps of 1°C per 30 mins. $T_{LCST}$ was taken as the temperature at which a sharp decrease in the transmittance occurs upon heating. $T_{LCST}$ = 22°C and 33°C was obtained for PNIBA and PNIPAM respectively (Figure S1). Note that some hysteresis was observed in the heating/cooling cycle, which is also reported in the literature.[7]

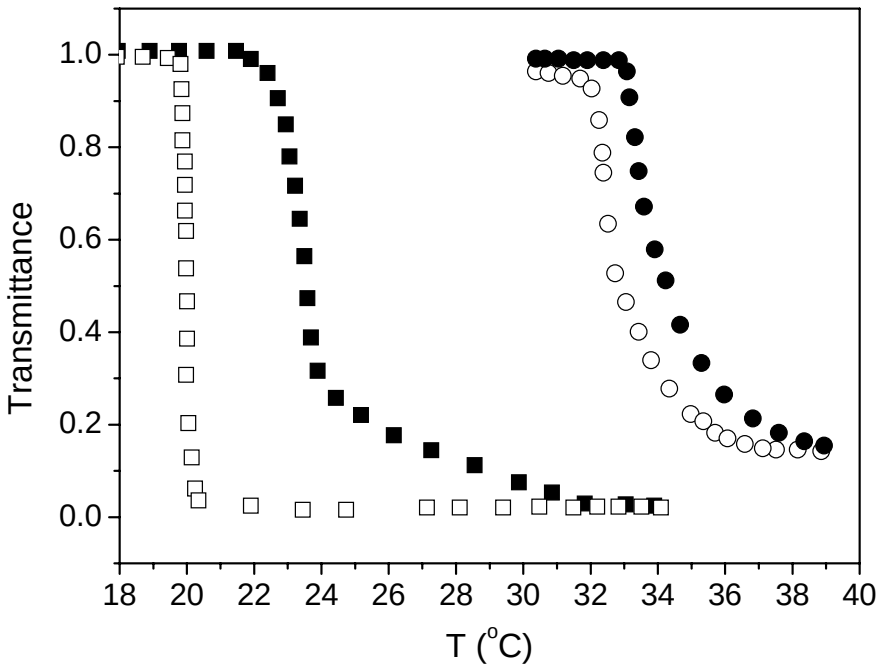


Figure S1. Transmittance versus temperature of the carboxyl-terminated polymer solutions. The concentration is 0.06% (m/v); the heating/cooling speed is 1°C per 30 mins. Circles: carboxyl group terminated poly(*N*-isopropylacrylamide) (PNIPAM); Squares: carboxyl group terminated poly(*N*-isopropylacrylamide-*co*-*N*-*tert*-butylacrylamide) (PNIBA); Full symbols: heating; Open symbols: cooling.

### 3.2 Characterization of *fd* grafted with polymers

***SDS-PAGE*** The main component of *fd* virus is a rod-like protein capsid, consisting of 2700 identical coat proteins—g8p. The solvent exposed part of g8p offers amino functional groups for grafting with polymers. With these properties, SDS-PAGE is a convenient way to analyze the chemical modification of *fd* virus.

SDS-PAGE was performed following the standard Laemmli method.[8] A gel with a density of 18% was used. Wild type or modified *fd* viruses were denatured in the buffer containing 1.6% SDS, 1% β-mercaptoethanol, 12.5% glycerol, 0.0025% bromophenol blue and 50mM Tris-HCl (pH 7.6) (final concentration). The resulting mixture of major coat proteins g8p, minor proteins, phage DNA and other agents were loaded onto the gel which was run under a buffer condition of 1% SDS, 1.92 mM glycine, 250 mM Tris (final concentrations). Commercially available molecular weight markers (Amersham Biosciences) were applied to one lane of the gel in order to estimate the

apparent molecular weight. Gels were stained with Coomassie Brilliant Blue R-250 for visualizing the protein bands.

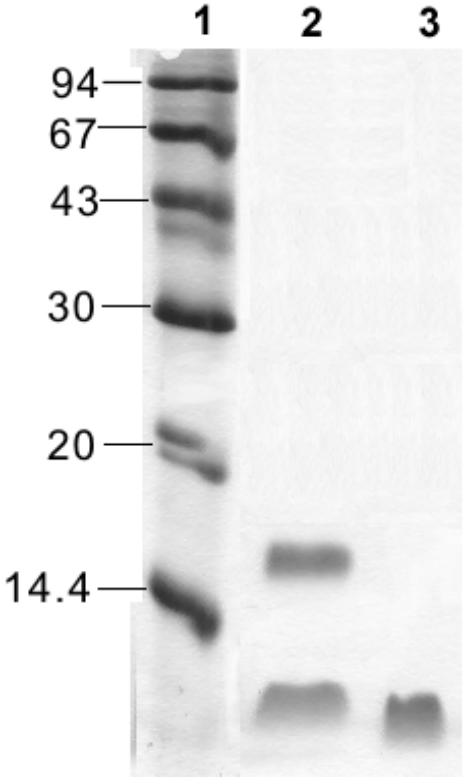


Figure S2. SDS-PAGE of PNIPAM-*fd* and wild type *fd*. Lane 1: molecular weight markers (x $10^3$ g $mol^{-1}$); Lane 2: PNIPAM-*fd*; Lane 3: wild type *fd*.

In Figure S2, besides the band corresponding to the coat protein—g8p, another band appears at the position of a higher molecular weight in the lane of PNIPAM-*fd*, which should be g8p grafted with PNIPAM. A molecular weight of 7k and 15k can be estimated for g8p and g8p grafted with PNIPAM respectively.[9] Assuming that each coat protein grafted with only one PNIPAM, an apparent molecular weight of ca. 8k for the grafted PNIPAM is obtained, which is comparable to the value estimated by the end function group titration.

***Isotropic-nematic (I-N) phase transition*** PNIPAM-*fd* was redispersed in Tris-HCl buffer to form concentrated suspensions of different ionic strengths (I). The suspensions were kept in a water-bath of temperature 20°C between crossed polarizers and birefringence was observed. The same Tris-HCl buffer was added in an amount of 5 μL per step until the birefringence just disappears.

The concentration of the resulted dispersions, denoted as $C_{I\text{-}N}$, was then determined by assuming that $C_{I\text{-}N}$ is equal to the concentration in the isotropic liquid phase coexisting with the nematic phase.

***Number of PNIPAM polymers per virus*** Since the refractive index increment (*dn/dc*) is proportional to the mass density, the *dn/dc* difference between the bare virus and the PNIPAM-*fd* is due to the grafted polymer. This can be used to estimate the number of grafted polymers on each virus.[10] The *dn/dc* of carboxyl-terminated PNIPAM ($(dn/dc)_p$) and *fd* virus ($(dn/dc)_{fd}$) were determined with the homemade scanning Michelson differential interferometer at T = 25°C [6]. As for PNIPAM-*fd* system, the concentration of *fd* virus in PNIPAM-*fd* suspensions can be easily obtained by UV absorption (PNIPAM does not absorb in the UV range where *fd* absorbs). So an apparent *dn/dc* can also be determined based on the virus concentration ($(dn/dc)_{app}$). The number of PNIPAM grafted on each virus, *N*, can be estimated by the following equation[10]:

$$N = \frac{(dn/dc)_{app} - (dn/dc)_{fd}}{(dn/dc)_p} \times \frac{M_w^{fd}}{M_w^p} \quad , \qquad \textbf{(1)}$$

with $M_w^{fd}$ and $M_w^p$ the molecular weight of *fd* ($1.64 \times 10^7$ g mol$^{-1}$) and of the polymer respectively.

Four samples with concentrations ranging from 0.001 to 0.005 g mL$^{-1}$ in pure water were prepared for carboxyl terminated PNIPAM, *fd* and PNIPAM-*fd*. The dn/dc values of 0.192, 0.172 and 0.165 mL g$^{-1}$ are obtained for PNIPAM-*fd*, *fd*, PNIPAM respectively. With equation (1), N ~ 300 is calculated, indicating that only a small portion of the coat proteins (g8p) are grafted with PNIPAM. This value is of the same order of magnitude as the amount of PEG found in the PEG5k-*fd* system (ca. 400 polymer per virus was reported)[10] and is also consistent with the SDS-PAGE result (see Figure S2).

**Estimation of the effective particle volume** Several effective diameters, $D_{eff}$, have been distinguished (See Fig.1C in the main text). The first is the diameter defined by the bare *fd* and the grafted polymer layer, $D_{eff}^{polymer}$. The second is the diameter defined by the electrostatic double layer, $D_{eff}^{electrostatic}$. For PNIPAM-*fd*, $D_{eff}^{polymer}$ should equal to the bare diameter of *fd* (6.6 nm) plus the thickness of the grafted PNIPAM layer. In this case, two situations emerge. When T < T*,

$D_{eff}^{polymer}$ equals the bare diameter of *fd* (6.6 nm) plus the $4R_g$ of the grafted PNIPAM in the coil conformation. $R_g$ is estimated to be 3 nm for PNIPAM of $M_w$ = 7k.[11] So $D_{eff}^{polymer} = D_{fd} + 4R_g = 19$ nm. When T > T*, $D_{eff}^{polymer}$ equals the bare diameter of *fd* plus $4R_g$ of the grafted PNIPAM in the globular conformation. $R_g$ is estimated to be 1 nm for $M_w$ of 7k. [11] In this case, $D_{eff}^{polymer} = D_{fd} + 4R_g = 10$ nm. The corresponding volume fraction can be calculated by $\Phi = C_{fd} N_A L \pi (D_{eff}/2)^2 / M_w$, with $N_A$ being the Avogadro's number and $M_w$ the molecular weight of *fd* virus.

## 4. Physical experiments

### 4.1 Determination of gel point by transmittance change upon varying temperature

Transmittance versus temperature of the suspensions of the virus grafted with polymers was monitored on the homemade scanning Michelson differential interferometer as described above.[6] For this, the dispersion of PNIPAM-*fd* or PNIBA-*fd* with a concentration of 3.5 mg $mL^{-1}$ and an ionic strength of 110 mM was subjected to a heating/cooling cycle with a heating/cooling speed of $1^oC$ per 30 mins. The gel point is defined as the temperature at which the transmittance decreases sharply.

### 4.2 Determination of gel point by test tube inversion experiments

In order to investigate the influence of ionic strength and concentration on the gel point, PNIPAM-*fd* was dispersed in Tris-HCl buffer, resulting in suspensions of different concentrations and ionic strengths. The glass vials containing these suspensions were immersed in a water bath with a temperature control with an accuracy of $\pm 0.01^oC$. The temperature was increased from $10^oC$ to $60^oC$ in steps of $1^oC$ per 10 min, and vice versa. The vials were equilibrated at each temperature for 30 min and then checked by inverting up down. The gel point, $T^*$, is defined as the temperature at which the dispersion stops flowing and a space-filling gel forms. The critical concentration was also defined in a similar way.

Two PNIPAM-*fd* suspensions of different ionic strengths (I) were investigated. One is a salt-free suspension (suspensions in deionized water), in which strong interparticle electrostatic repulsions

are expected. Another one is a suspension of I = 110 mM, in which the electrical double layer is confined into the PNIPAM layer so that the steric repulsion by the polymer in a good solvent ($T < T^*$) is dominant. The results are summarized in Tables 1 and 2. The gelation point weakly depends on the concentration, especially in the case of salt-free suspension. For both dispersions, there exists a critical concentration $C^*$, above which gelation occurs. Note that the gel point is consistent with that determined by the transmittance method (see the main text).

Table 1. Gelation behavior of salt-free PNIPAM-*fd* suspension at different concentrations

| C (mg $mL^{-1}$)* | Gelation phenomena | Gel point ($^oC$) |
|---|---|---|
| 7.80 | Translucent gel, birefringence | 33 |
| 3.70 | Translucent gel, birefringence | 35 |
| 2.21 | Weak Gel | 36 |
| 1.85 | Weak Gel | 38 |
| 0.94 | No gelation occurs even by heating up to 60 $^oC$ | — |

* Concentration of *fd* virus in the PNIPAM-*fd* suspension.

Table 2. Gelation behavior of PNIPAM-*fd* suspension at I = 110 mM and at different concentrations

| C (mg $mL^{-1}$)* | Gelation phenomena | Gel point ($^oC$) |
|---|---|---|
| 7.80 | Turbid gel, No birefringence | 33 |
| 3.91 | Translucent gel, No birefringence | 33 |
| 1.84 | Translucent gel, No birefringence | 34 |
| 0.90 | Weak gel | 34 |
| 0.76 | Weak gel / very viscous fluid | 34 |
| 0.4 | No gelation occurs even by heating up to 60 $^oC$ except that the suspension becomes viscous | — |

* Concentration of *fd* virus in the PNIPAM-*fd* suspension.

**4.3 Rheological experiments**

4.3.1 Background

The gelation behavior of the PNIPAM-*fd* was subjected to rheological investigation with a strain-controlled rheometer (ARES, TA instruments, De, USA). The rheometer is equipped with a

sensitive force rebalanced transducer (100 g.cm torque). A cone and plate geometry was used with a 50 mm diameter and an angle of 0.04 radian, to ensure a homogenous deformation throughout the sample. Temperature control was carried out by a Peltier element. The sample was allowed to equilibrate at each temperature for 60s prior to the measurements. A double vapor lock solvent trap was used as to minimize solvent evaporation. Strain sweeps at frequencies of 1 and 5 rad/s were conducted at different temperatures (above and below gel point) to determine the linear regime and the minimal linearity limit which is obeyed at all temperatures. Subsequently a frequency sweep was performed at a particular strain % below the minimal linearity limit.

The rheological definition of the gel point is that the relaxation modulus is described by a simple power law: $G(t) = St^{-n}$. For the dynamic moduli this implies that, at the gel point, both the storage ($G'$) and the loss ($G''$) modulus are power laws over the whole frequency range. Hence at the gel point, the phase angle ($\delta$, $\delta = \tan^{-1}(G''/G')$) is independent of frequency. The Winter-Chambon method consists in monitoring $\tan(\delta)$, or the change of $\tan(\delta)$ ($\Delta\tan(\delta)$) with respect to frequency. The latter should be close to zero near the gel point.[12]

4.3.2 Method for determination of the gel point

To determine the gel point, oscillatory frequency sweep experiments were performed at a strain% in the linear regime for different temperatures. Figure S3 shows $\tan(\delta)$ as a function of frequency for a 3 mg $mL^{-1}$ PNIPAM-*fd* suspension. In the sol state, the inertial contribution of the instrument to the measurements limits the frequency range to about 10 rad/s. At temperatures 27 to 32$^{o}$C the sample is in the isotropic sol state, the slope of $\tan(\delta)$ is negative and depends on the frequency. Between 32 and 33°C the modulus increases and $\tan(\delta)$ becomes independent of frequency, identifying the critical gel point.

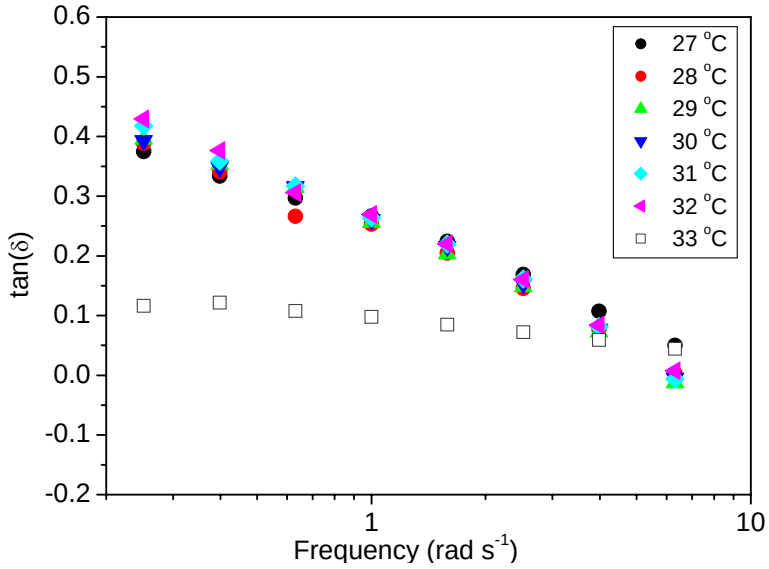


Figure S3. Oscillatory frequency sweeps at a strain of 1% and at different temperatures for a 3 mg $mL^{-1}$ PNIPAM-*fd* suspension at I = 110 mM.

Moreover, the transition to the gel state is also characterized by an increase of the magnitude of storage moduli and a decrease of the phase angle. Figure S4 shows absolute values of G' and phase angle (δ) as a function of temperature for a 3 mg $mL^{-1}$ PNIPAM-*fd* suspension. There is a large increase in G' and a drop in δ in the range of 32 to 33°C.

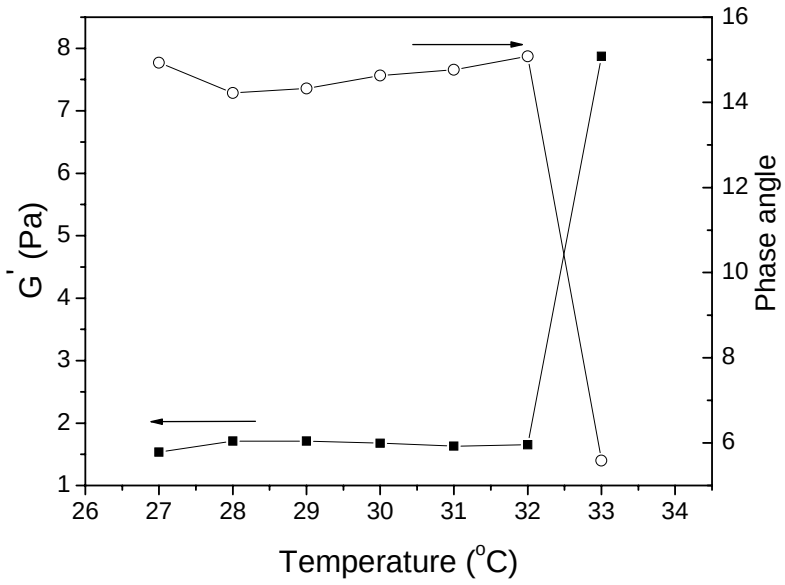


Figure S4. Storage moduli (G') and phase angle (δ) versus temperature for 1% strain at a frequency of 1 rad/s. The sample is the same as described in Figure S3.

The accurate gelation points were determined by plotting Δtan(δ) against the temperature for the

two PNIPAM-*fd* suspensions described in the main text (C = 8.5 mg $mL^{-1}$, I = 5 mM and 110 mM respectively). The gel points are determined by taking the temperature at which Δtan(δ) is zero. In the case of 110 mM the gel point is at 33.2°C and for 5mM it is 35.2°C.

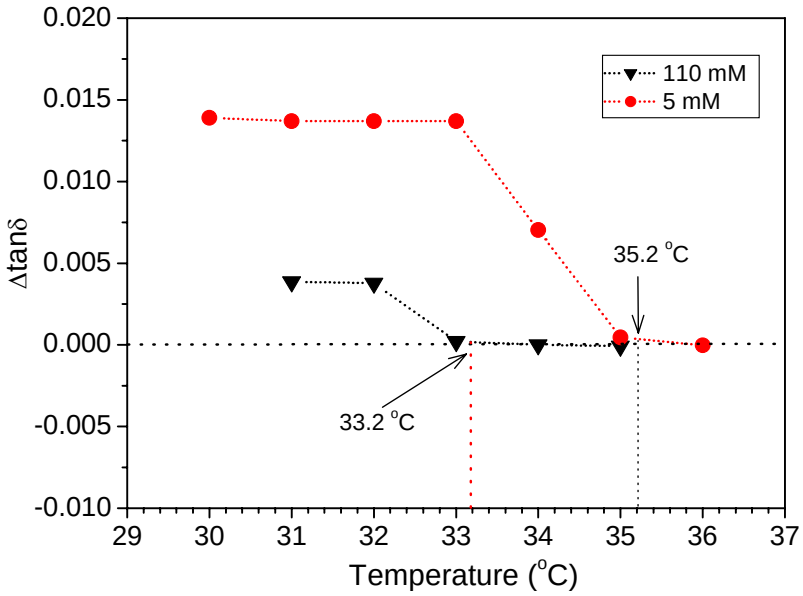


Figure S5. Δtan(δ) (at 1 rad/s) vs temperature for PNIPAM-*fd* suspensions of C = 8.5mg $mL^{-1}$ and at I = 5 mM or 110 mM.

### 4.4 SAXS experiment

A lab SAXS setup (NanoStar Bruker AXS) was used. The beam of the anode x-ray generator had a size of about 500 μm and a wavelength of 1.54 Å. The sample-to-detector distance was 1.1 m. The temperature was controlled by a water circulating bath incorporated into the sample holder. PNIPAM-*fd* suspensions were injected into 1.5 mm quartz x-ray capillaries and sealed by flame.

### 4.5 Optical microscopy

Birefringence was checked with an Olympus BX51 optical microscope equipped with cross polarizers. The PNIPAM-*fd* suspensions were injected into 1.5 mm cylindrical glass capillaries and then immersed into the mini water pool of a home-made heating plate. Water was used for homogeneous heat conducting and for index matching to correct optical distortions produced by the cylindrical capillary. The images were recorded by a CCD camera.

For magnetic alignment, the capillaries containing the liquid crystalline PNIPAM-*fd* suspensions were put into a 7T magnetic filed of an NMR setup for 24 hrs. Alignment of the samples was checked by optical microscopy. Samples of high degree of alignment were further subjected to

quick heating/cooling, during which the optical retardation, *R*, was measured with a 3λ Berek compensator. Birefringence Δn was then calculated by Δn = R/d, where d is the sample thickness within the capillary.[13]

# References


(1) (a) Takei, Y. G.; Aoki, T.; Sanui, K.; Ogata, N.; Okano, T.; Sakurai, Y. *Bioconjugate Chem.* 1993, *4*, 42-46. (b) Ding, Z. L.; Chen, G. H.; Hoffman, A. S. *Bioconjugate Chem.* 1996, *7*, 121-125.

(2) Chen, G.; Hoffamn, A. S. *J. Biomater. Sci. Polymer Edn.* 1994, *5*, 371-382.

(3) Miron, T.; Wilchek, M. *Anal. Biochem.* 1982, *126*, 433-435.

(4) Sambrook, J.; Russell, D. W. *Molecular Cloning: A Laboratory Manual*; 3 ed.; Cold Spring Harbor Laboratory Press: New York, 2001.

(5) Berkowitz, S. A.; Day, L. A. *J. Mol. Biol.* 1976, *102*, 531-547.

(6) Becker, A.; Kohler, W.; Muller, B. *Ber. Bunsen-Ges. Phys. Chem. Chem. Phys.* 1995, *99*, 600-608.

(7) Cheng, H.; Shen, L.; Wu, C. *Macromolecules* 2006, *39*, 2325-2329; Sun, B.; Lin, Y.; Wu, P.; Siesler, H. W. *Macromolecules* 2008, *41*, 1512-1520.

(8) Laemmli, U. K. *Nature* 1970, *227*, 680-685.

(9) Schwind, P.; Kramer, H.; Kremser, A.; Ramsberger, U.; Rasched, I. *Eur. J. Biochem.* 1992, *210*, 431-436.

(10) Grelet, E.; Fraden, S. *Phys. Rev. Lett.* 2003, *90*, 198302.

(11) Wu, C.; Wang, X. H. *Phys. Rev. Lett.* 1998, *80*, 4092.

(12) Chambon, C.; Petrovic, Z. S.; MacKnight, W. J.; Winter, H. H. *Macromolecules* 1986, *19*, 2146-2149.

(13) Purdy, K. R.; Dogic, Z.; Fraden, S.; Ruhm, A.; Lurio, L.; Mochrie, S. G. J. *Phys. Rev. E* 2003, *67*, 031708.